Orientation and Restricted Rotation of Lopsided N-Donor Heterocyclic Bioligands in Octahedral Ruthenium Complexes

Enzo Alessio,*[a] Elisabetta Iengo,[a] Ennio Zangrando,[a] Silvano Geremia,[a] Patricia A. Marzilli,[b] and Mario Calligaris[a]

Keywords: Ruthenium / Dimethyl sulfoxide / N ligands / Molecular dynamics / Atropisomerism / Bioinorganic chemistry

In order to analyze the roles of steric and electrostatic factors in determining the orientation and dynamic behavior of benzimidazole-type ligands in Ru^{II}(dimethyl sulfoxide) complexes, compounds of the general formula $RuX_2(dmso\text{-}S)_{2-n}(CO)_n(L)_2$ [X = Cl, Br; L = 1,5,6-trimethylbenzimidazole (Me_3Bzm), benzimidazole (Bzm); n = 0–2] with *cis* and *trans* arrangements of the X ligands, have been prepared and structurally characterized both in solution and in the solid state, by NMR and X-ray techniques, respectively. New descriptors, based on the torsion angles about the Ru–N bonds, are introduced for a more efficient definition of the head-to-head (HH) and head-to-tail (HT) orientations of the heterocyclic nitrogen bases. Similar descriptors, based on the torsion angles about the Ru–S bonds, are used to define the orientation of the dimethyl sulfoxide ligands. The experimental molecular conformations are discussed on the basis of molecular mechanics (MM) calculations. The electrostatic interaction between the halide ligands and the positively charged N_2CH proton on the imidazole ring has been found to be the essential factor in determining the specific orientation of one Me_3Bzm base, both in the solid state and in solution. The different stabilities of the HH and HT base conformations observed in solution, in the solid state, and in the isolated molecules are rationalized in terms of solvation and packing effects. The larger solvent-accessible surface area in the HH conformation as compared with that in the HT form leads to more effective intermolecular interactions, which are responsible for stabilizing the former geometry in the condensed phase.

Introduction

The *cis*-M(L1)(L2) unit, where L1 and L2 are either the same or different planar aromatic N-donor ligands, is a common motif in biological systems, in particular in cross-links formed by DNA with metal anticancer drugs and in metalloenzymes.[1] These units are usually highly dynamic and difficult to evaluate in solution. Consequently, there have been relatively few cases where rotation of the L1 and L2 ligands about the M−N bond has proved to be sufficiently slow for structural and dynamic features to be assessed.[2−8] We have found that improved insight into the features of such units can be gained by studying complexes of the bioligand 1,5,6-trimethylbenzimidazole (Me_3Bzm) (Scheme 1) and comparing the results of studies on analogs with the non-biological pyridine ligands. Various types of information can be gained since bioligands are typically non-C_2-symmetric (i.e. lopsided), whereas the selected non-biological ligands are C_2-symmetric. When both ligands in the *cis*-M(L1)(L2) unit are lopsided, there are four possible major rotamers: two with head-to-head (HH) orientation and two with head-to-tail (HT) orientation (Scheme 2). When only one ligand is lopsided, there are two rotamers. When neither ligand is lopsided, there is only one possible rotamer. If the lopsided ligands L1 and L2 are identical, and the metal center and "spectator" (also called carrier) ligands form a highly symmetric carrier ligand−metal center moiety, only one HH rotamer is possible. One further feature is that some of the HT rotamers may be enantiomers.

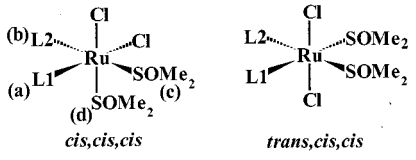

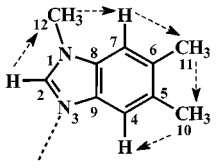

Scheme 1. Schematic representation of the generic octahedral *c*,*c*,*c*-$RuCl_2(dmso\text{-}S)_2(L1)(L2)$[9] (left, with labeling scheme of ligand positions) and *t*,*c*,*c*-$RuCl_2(dmso\text{-}S)_2(L1)(L2)$[9] (right) isomers; in this work L1 = L2 = Me_3Bzm (bottom, showing numbering scheme and intraligand NOE connectivity path), while either one or both dmso-S ligands may be replaced by CO

We recently reported that restricted rotation about Ru−N bonds in octahedral complexes of the type *cis*,*cis*,*cis*-$RuCl_2(dmso\text{-}S)_2(L1)(L2)$[9] (L1 *trans* to Cl, L2 *trans* to dmso-S; Scheme 1) allows assessment of the relative ori-

[a] Dipartimento di Scienze Chimiche, Università di Trieste, Via Giorgieri 1, 34127 Trieste, Italy
E-mail: alessi@univ.trieste.it
[b] Department of Chemistry, Emory University, Atlanta, GA 30322, USA
Supporting information for this article is available on the WWW under http://www.wiley-vch.de/home/eurjic or from the author.

  1434−1948/00/1010−2207 $ 17.50+.50/0

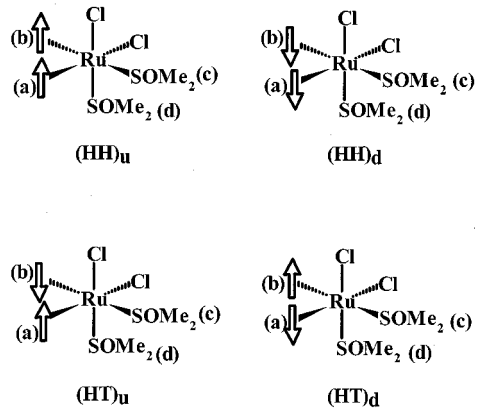

Scheme 2. Schematic representation of the four possible major rotamers of *c*,*c*,*c*-$RuCl_2$(dmso-S)$_2$(Me_3Bzm)$_2$ (**1**); Me_3Bzm is indicated with an arrow, with the head corresponding to B2H

entation and dynamic motion of two *cis*-coordinated N-donor aromatic ligands. The use of C_2-symmetric ligands, such as pyridine (py) and 3,5-lutidine (3,5-lut), in combination with non-C_2-symmetric ligands such as Me_3Bzm and 1,2-dimethylimidazole (1,2-Me_2Im) provides more insight than the use of either type alone.[1−5,8] NMR investigations of the dynamic behavior of such compounds in solution showed that, at ambient temperature, they exist in a definite number of conformers that are in an essentially slow-exchange equilibrium, the position of which depends on the nature of the nitrogen bases.

The results obtained with Me_3Bzm were particularly significant as they indicated that its dynamic behavior was strongly influenced not only by steric factors, but also by electrostatic interactions.[1] In Me_3Bzm, which is a nucleopurine analog, the N_2CH proton on the imidazole ring (B2H) is relatively acidic and hence bears a partial positive charge (δ+), which is increased upon coordination to metal centers. We found that in ruthenium(II)[1−5] and rhenium(V)[8] Me_3Bzm complexes, the electrostatic attraction between the $N_2CH^{\delta+}$ proton(s) and the negative ligands (e.g. oxo, Cl) is important in determining the observed conformations. In particular, the solid-state structures of *c*,*c*,*c*-$RuCl_2$(dmso-S)$_2$(Me_3Bzm)$_2$, *c*,*c*,*c*-$RuCl_2$(dmso-S)$_2$(1,2-Me_2Im)(Me_3Bzm), and *c*,*c*,*c*-$RuCl_2$(dmso-S)$_2$(py)(Me_3Bzm) showed that the Me_3Bzm *trans* to dmso-S has the same orientation in the three complexes, with the mean plane of the ligand almost bisecting the Cl−Ru−Cl angle and B2H almost equidistant from the two Cl atoms. Moreover, for *c*,*c*,*c*-$RuCl_2$(dmso-S)$_2$(1,2-Me_2Im)(Me_3Bzm) and *c*,*c*,*c*-$RuCl_2$(dmso-S)$_2$(py)(Me_3Bzm) we found no evidence of the other possible geometrical isomer, i.e. that with Me_3Bzm *trans* to Cl. In solution, extensive NMR investigations provided strong evidence that, at ambient temperature, the Me_3Bzm *trans* to dmso-S remains relatively fixed, maintaining an orientation very similar to that found in the solid state; the dynamic behavior of the other N-donor ligand depends on its nature.[2−4] In *c*,*c*,*c*-$RuCl_2$(dmso-S)$_2$(Me_3Bzm)$_2$, the Me_3Bzm *trans* to Cl slowly (on the NMR time scale) flips between two orientations at ca. 180°, thus generating one HH and one HT rotamer of almost equal stability. Only the rare (at the time) HH atropisomer was found in the solid state.[2,3]

The imidazole ring is a common feature of many biological ligands. The electrostatic interaction between the $N_2CH^{\delta+}$ proton and the other ligands is likely to be of general relevance for all those biological systems in which metal sites are bound to imidazole rings (e.g. B_{12} systems, Pt drug adducts of DNA, metalloenzymes, and metalloproteins).[1]

In order to analyze in greater detail the roles of steric and electrostatic factors in determining the orientation and dynamic behavior of the Me_3Bzm ligand, we have prepared and studied some new Me_3Bzm (and Bzm) Ru^{II} compounds closely related to those mentioned above. As compared to the thoroughly investigated complex *c*,*c*,*c*-$RuCl_2$(dmso-S)$_2$(Me_3Bzm)$_2$ (**1**), we have changed the nature of the halogen (Br vs. Cl), the geometry of the complex (*trans*,*cis*,*cis* vs. *cis*,*cis*,*cis*),[9] and the number of dmso-S ligands (replaced by CO molecules). Thus, we have prepared and investigated on the basis of NMR and X-ray structural data in conjunction with molecular mechanics (MM) calculations, the two series of geometrical isomers of the formula *cis*,*cis*,*cis*- and *trans*,*cis*,*cis*-RuX_2(dmso-S)$_{2-n}$(CO)$_n$(L)$_2$ [X = Cl, Br; L = 1,5,6-trimethylbenzimidazole (Me_3Bzm), benzimidazole (Bzm); n = 0−2]. In particular, the compounds reported here are: *c*,*c*,*c*-$RuBr_2$(dmso-S)$_2$(Me_3Bzm)$_2$ (**2**), *t*,*c*,*c*-$RuCl_2$(dmso-S)$_2$(Me_3Bzm)$_2$ (**3**), *t*,*c*,*c*-$RuCl_2$(dmso-S)$_2$(Bzm)$_2$ (**4**), *c*,*c*,*c*-$RuCl_2$(dmso-S)(CO)(Me_3Bzm)$_2$ (**5**), *t*,*c*,*c*-$RuCl_2$(dmso-S)(CO)(Me_3Bzm)$_2$ (**6**), and *c*,*c*,*c*-$RuCl_2$(CO)$_2$(Me_3Bzm)$_2$ (**7**). Finally, with the aim of establishing whether the polarity of the medium of crystallization and/or packing interactions might affect the solid-state molecular conformation, we recrystallized **1** from hot benzene rather than from dmso/acetone mixtures,[3] which furnished crystals of *c*,*c*,*c*-$RuCl_2$(dmso-S)$_2$(Me_3Bzm)$_2$·2C_6H_6 (**8**). The crystal structure of **8** has been determined, as have those of **2**−**6**.

Results

Crystal and Molecular Structures

Coordination distances and sulfoxide bond lengths and angles for complexes **2**−**6** and **8** (Table 1 and 2) fall well within the ranges of values found in Ru^{II} compounds.[10] Merging the present data with those reported previously, mean values of 2.139(6) and 2.440(4) Å are obtained, respectively, for the Ru−N and Ru−Cl distances *trans* to sulfur, while those not *trans* to sulfur amount to 2.110(4) and 2.417(4) Å, respectively. The observed lengthenings of 0.029 Å (Ru−N) and 0.023 Å (Ru−Cl) confirm the *trans* influence of *S*-bonded dmso on the relevant Ru−N and Ru−Cl bonds.[10a] The Ru−C and Ru−S bond lengths in the carbonyl derivatives [1.832(6) and 2.284(1) Å, respectively, in **5**; 1.843(4) and 2.284(1) Å in **6**] are close to those reported for Ru^{II}(monocarbonyl)(dmso-S) complexes.[11] Interestingly, the Ru−S distances in **5** and **6** [2.284(1) Å] are significantly longer than those in **1**−**4** and **8** [av. 2.248(3) Å], as would be expected following the introduc-

tion of a strong π acceptor ligand into the coordination sphere.[11] Furthermore, the previously observed deformation of the Ru−N−C bond angles in benzimidazole complexes is also fully confirmed here. In fact, the average Ru−N(1)−C(5), Ru−N(1)−C(14), Ru−N(2)−C(15), and Ru−N(2)−C(24) bond angles measure 123.6(8)°, 130.8(6)°, 120.5(3)°, and 134.3(5)°, respectively, in agreement with previous data.[2,3,5]

Table 1. Selected bond lengths [Å] and angles [°] for compounds *c*,*c*,*c*-$RuBr_2$(dmso-S)$_2$(Me_3Bzm)$_2$ (**2**), *c*,*c*,*c*-$RuCl_2$(dmso-S)(CO)(Me_3Bzm)$_2$ (**5**), and *c*,*c*,*c*-$RuCl_2$(dmso-S)$_2$(Me_3Bzm)$_2$·$2C_6H_6$ (**8**)

	2	**5**	**8**
Distances	L = S(2), X = Br	L = C(3), X = Cl	L = S(2), X = Cl
Ru−N(1)	2.118(5)	2.109(4)	2.103(2)
Ru−N(2)	2.145(6)	2.115(4)	2.135(2)
Ru−S(1)	2.249(2)	2.284(1)	2.2484(9)
Ru−L	2.256(2)	1.832(6)	2.2415(8)
Ru−X(1)	2.5635(9)	2.393(1)	2.4326(9)
Ru−X(2)	2.589(1)	2.448(2)	2.4419(9)
S(1)−O(1)	1.473(6)	1.465(5)	1.479(3)
L−O(2)	1.478(5)	1.147(8)	1.472(2)
Angles			
X(1)−Ru−X(2)	89.17(4)	88.17(6)	88.40(3)
X(1)−Ru−S(1)	91.79(5)	89.27(5)	93.88(4)
X(1)−Ru−L	87.53(5)	88.9(2)	87.62(3)
X(1)−Ru−N(1)	175.8(2)	175.6(1)	175.02(7)
X(1)−Ru−N(2)	89.0(2)	89.3(1)	88.02(7)
S(1)−Ru−L	96.54(7)	93.3(2)	96.80(3)
S(1)−Ru−N(1)	91.1(2)	92.2(1)	89.29(7)
S(1)−Ru−N(2)	174.3(2)	178.6(1)	172.95(7)
L−Ru−N(1)	95.2(2)	95.1(2)	95.82(7)
L−Ru−N(2)	89.1(2)	86.4(2)	90.05(7)
N(1)−Ru−N(2)	87.9(2)	89.2(2)	88.4(1)
Ru−N(1)−C(5)	120.1(5)	123.5(4)	120.3(2)
Ru−N(1)−C(11)	134.2(4)	130.7(4)	134.6(2)
Ru−N(2)−C(12)	122.0(5)	124.8(4)	121.4(2)
Ru−N(2)−C(18)	131.7(5)	129.5(3)	132.4(2)
Ru−S(1)−O(1)	120.1(2)	118.8(2)	121.2(1)
Ru−S(1)−C(1)	112.6(3)	111.3(3)	110.7(1)
Ru−S(1)−C(2)	114.1(3)	12.3(3)	111.9(1)
C(1)−S(1)−C(2)	98.2(4)	96.9(5)	99.0(2)
Ru−L−O(2)	119.4(2)	173.2(6)	119.3(1)
Ru−L−C(3)	114.7(3)	−	113.6(1)
Ru−L−C(4)	110.7(3)	−	111.2(1)
C(3)−L−C(4)	98.0(4)	−	97.5(2)

A summary of the solid-state conformational parameters for the RuX_2(dmso-S)$_2$(L1)(L2) (X = Cl, Br; L1, L2 = Me_3Bzm, Bzm, or 1,2-Me_2Im) and $RuCl_2$(dmso-S)(CO)(Me_3Bzm)$_2$ complexes is given in Table 3 (see Discussion for conformation descriptors). These data show that, in spite of the presence of benzene molecules of crystallization, the molecular structure of the complex *c*,*c*,*c*-$RuCl_2$(dmso-S)$_2$(Me_3Bzm)$_2$ in **8** is comparable to that in **1**. Analogously, the molecular conformation of the bromo derivative *c*,*c*,*c*-$RuBr_2$(dmso-S)$_2$(Me_3Bzm)$_2$ (**2**) is very similar to that of **1**, and is practically unaffected by the presence of ethanol molecules in the lattice. The same labeling scheme has been used for the RuX_2(dmso-S)$_{2-n}$(CO)$_n$(Me_3Bzm)$_2$ moiety in all the complexes (X = Cl or Br, n = 0−2), as illustrated in Figures 1, 2 and 3, which show the molecular structures of **2**, **3**, **5**, and **6**.

Table 2. Selected bond lengths [Å] and angles [°] for compounds *t*,*c*,*c*-$RuCl_2$(dmso-S)$_2$(Me_3Bzm)$_2$ (**3**), *t*,*c*,*c*-$RuCl_2$(dmso-S)$_2$(Bzm)$_2$ (**4**), and *t*,*c*,*c*-$RuCl_2$(dmso-S)(CO)(Me_3Bzm)$_2$ (**6**)

	3	**4**	**6**
Distances	L = S(2)	L = S(2)	L = C(3)
Ru−N(1)	2.177(2)	2.155(3)	2.168(3)
Ru−N(2)	2.134(2)	2.128(3)	2.112(3)
Ru−S(1)	2.2402(9)	2.2349(9)	2.284(1)
Ru−L	2.2604(8)	2.2673(9)	1.843(4)
Ru−Cl(1)	2.4128(9)	2.4054(9)	2.388(1)
Ru−Cl(2)	2.4117(9)	2.4309(9)	2.404(1)
S(1)−O(1)	1.478(3)	1.482(3)	1.474(3)
L−O(2)	1.475(3)	1.482(2)	1.132(5)
Angles			
Cl(1)−Ru−Cl(2)	177.57(3)	177.19(3)	177.81(4)
Cl(1)−Ru−S(1)	93.85(3)	94.93(3)	91.36(4)
Cl(1)−Ru−L	86.05(3)	84.24(3)	90.0(2)
Cl(1)−Ru−N(1)	94.02(7)	94.58(7)	87.11(9)
Cl(1)−Ru−N(2)	90.73(7)	89.73(7)	87.71(9)
S(1)−Ru−L	93.50(3)	93.80(3)	93.5(2)
S(1)−Ru−N(1)	91.32(7)	93.14(8)	87.90(9)
S(1)−Ru−N(2)	174.38(7)	174.89(7)	173.62(9)
L−Ru−N(1)	175.16(7)	173.04(7)	176.8(2)
L−Ru−N(2)	90.07(7)	88.74(7)	92.8(2)
N(1)−Ru−N(2)	85.09(9)	84.4(1)	85.8(1)
Ru−N(1)−C(5)	119.2(2)	121.1(2)	123.3(3)
Ru−N(1)−C(11)	135.9(2)	133.7(2)	130.5(2)
Ru−N(2)−C(12)	124.7(2)	123.7(2)	121.6(3)
Ru−N(2)−C(18)	130.2(2)	129.9(2)	132.3(3)
Ru−S(1)−O(1)	119.3(1)	117.2(1)	117.1(1)
Ru−S(1)−C(1)	110.5(1)	111.2(2)	111.3(2)
Ru−S(1)−C(2)	114.4(1)	116.5(2)	113.3(2)
C(1)−S(1)−C(2)	98.4(2)	98.9(2)	100.6(3)
Ru−L−O(2)	115.8(1)	114.4(1)	178.8(5)
Ru−L−C(3)	113.8(2)	115.5(2)	−
Ru−L−C(4)	114.7(1)	115.6(1)	−
C(3)−L−C(4)	98.6(2)	98.2(2)	−

Solution Studies

For the sake of clarity, the labeling schemes for the coordination positions of the ligands[9] and for the Me_3Bzm protons (Scheme 1) used in this work are the same as those used in our previous reports.[1−5] In particular, we label the base *trans* to Cl as "a", the base *trans* to S as "b", and the dmso ligands *trans* to "b" and Cl as "c" and "d", respectively.

cis,cis,cis Compounds

cis,cis,cis-$RuCl_2$(dmso-S)(CO)(Me_3Bzm)$_2$ (**5**)

This complex can be thought of as being formally derived from **1** through the replacement of dmso-S "d" by CO (Scheme 3). The ^{1}H NMR spectrum of **5** shows only one set of peaks for each non-equivalent Me_3Bzm ligand and one resonance for each diastereotopic dmso-S methyl group (Figure 4), as expected for an unsymmetrical *cis,cis,cis* complex. All resonances are sharp and no evidence for conformational equilibria due to hindered rotation of the nitrogen ligands is apparent at room temperature.

Table 3. Base and dmso solid-state conformational parameters, Ψ and Φ [°], with their diastereotopomer descriptors of some *c*,*c*,*c*- and *t*,*c*,*c*-$RuX_2(dmso\text{-}S)_{2-n}(CO)_n(L1)(L2)$ complexes, with X = Cl, Br; *n* = 0, 1; L1, L2 = Me_3Bzm, Bzm, 1,2-Me_2Im

Complex		Ψ_a	Ψ_b	base		Φ	Ψ_c	Ψ_d	dmso	
Δ *c*,*c*,*c*-$RuCl_2(dmso\text{-}S)_2(Me_3Bzm)_2$ [a]	**1**	−45.8	131.5	$(HH)_u$	H_4H_2	47.7	−13.7	83.6	$(HH)_d$	$H_0H_{\pi/2}$
Δ *c*,*c*,*c*-$RuCl_2(dmso\text{-}S)_2(Me_3Bzm)_2{\cdot}2C_6H_6$ [b]	**8**	−48.2	136.1	$(HH)_u$	H_4H_2	48.5	−11.5	90.4	$(HH)_d$	$H_0H_{\pi/2}$
Δ *c*,*c*,*c*-$RuBr_2(dmso\text{-}S)_2(Me_3Bzm)_2$ [a]	**2**	−44.9	138.1	$(HH)_u$	H_4H_2	45.8	−2.5	91.3	$(HH)_d$	$H_0H_{\pi/2}$
Δ *c*,*c*,*c*-$RuCl_2(dmso\text{-}S)_2(1,2\text{-}Me_2Im)(Me_3Bzm)$ [c]		129.1	136.5	$(HT)_d$	H_2H_2	43.8	−26.0	80.2	$(HH)_d$	H_4H_1
Δ *c*,*c*,*c*-$RuCl_2(dmso\text{-}S)(CO)(Me_3Bzm)_2{\cdot}0.5MeOH$ [b]	**5**	−57.2	144.2	$(HH)_u$	H_4H_2	68.3[d]	−92.0[e]			
t,*c*,*c*-$RuCl_2(dmso\text{-}S)_2(Me_3Bzm)_2$ [b]	**3**	−74.5[f]	126.2	HH	H_4H_2	78.6	29.1	161.7	HT	H_2H_1
t,*c*,*c*-$RuCl_2(dmso\text{-}S)_2(Bzm)_2$ [b]	**4**	−58.0[f]	127.3	HH	H_4H_2	54.4	32.4	159.9	HT	H_2H_1
t,*c*,*c*-$RuCl_2(dmso\text{-}S)(CO)(Me_3Bzm)_2$ [b]	**6**	123.0	−36.9	HH	H_2H_4	61.3	−108.6[e]			

[a] Ref.[3] – [b] Present work. – [c] Ref.[4] – [d] Mean value between the two locations of the Me_3Bzm ligand. – [e] Torsion angle C(3)−Ru−S(1)−O(1), C(3) substituting S(2). – [f] Bases "a" and "b" are exchangeable, and consequently so are dmso "c" and "d".

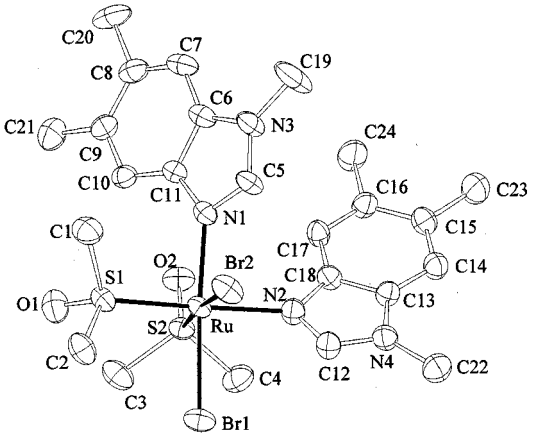

Figure 1. Molecular structure of the compound *c*,*c*,*c*-$RuBr_2(dmso\text{-}S)_2(Me_3Bzm)_2$ (**2**) (thermal ellipsoids drawn at a 40% probability level); the same scheme also applies to **8**, substituting the bromine atoms with chlorine atoms

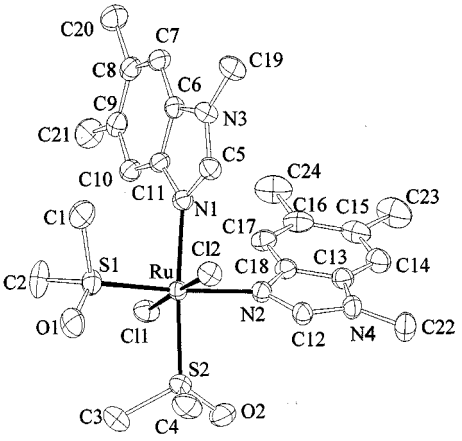

Figure 2. Molecular structure of the compound *t*,*c*,*c*-$RuCl_2(dmso\text{-}S)_2(Me_3Bzm)_2$ (**3**) (thermal ellipsoids drawn at a 40% probability level); the same scheme also applies to **4** with the exclusion of methyl groups C(19)−C(24)

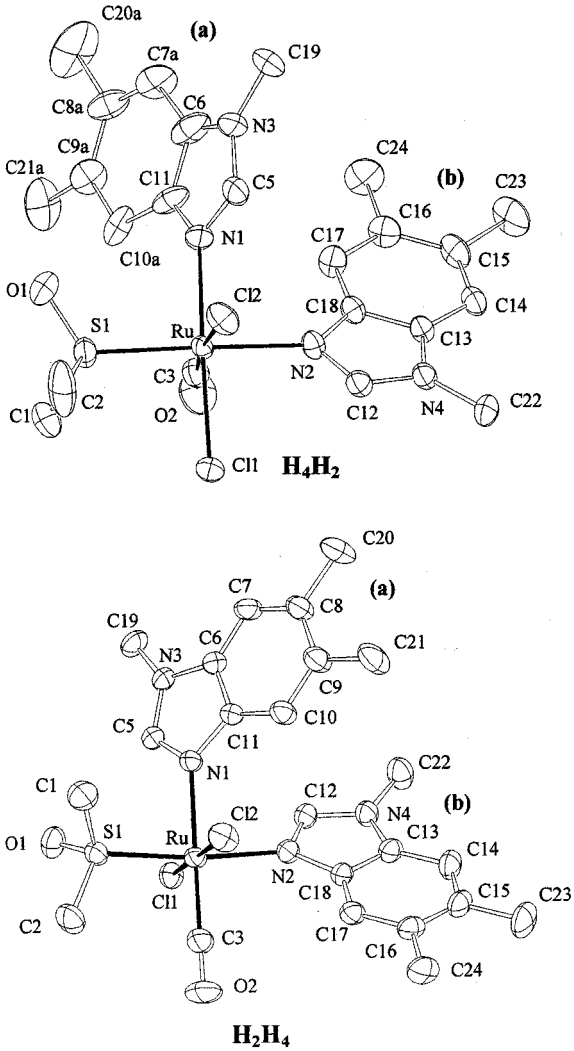

Figure 3. Molecular structures of the compounds *c*,*c*,*c*-$RuCl_2(dmso\text{-}S)(CO)(Me_3Bzm)_2$ (**5**) (top) and *t*,*c*,*c*-$RuCl_2(dmso\text{-}S)(CO)(Me_3Bzm)_2$ (**6**) (bottom, thermal ellipsoids drawn at a 40% probability level) with the relative conformational descriptors

Even though two isomers with a *cis*,*cis*,*cis* geometry are possible, depending on whether CO is *trans* to Cl or to Me_3Bzm, we isolated exclusively the compound in which CO is *trans* to Cl (as confirmed by the X-ray structure, see below) and found no evidence to suggest the existence of the other isomer. The resonances were assigned with the aid of a NOESY spectrum (Table 4); the intra-ligand NOE connectivity path ($B2H-B12H_3-B7H-B10H_3-B11H_3-B4H$; Scheme 1) allowed designation of the signals arising from each Me_3Bzm moiety, while the final assignment of the Me_3Bzm position as either "a" (i.e. *cis* to the dmso-S) or "b" (i.e. *trans* to dmso-S) was accomplished through the inter-ligand NOE contacts. In particular, from

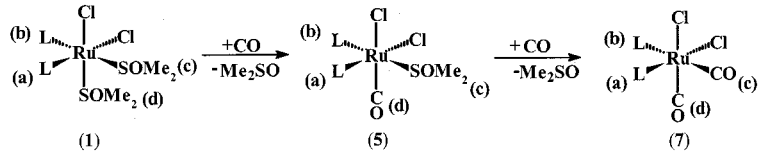

Scheme 3

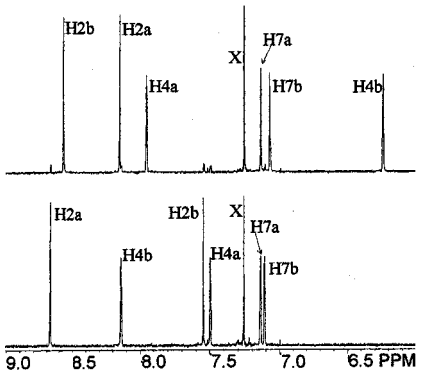

Figure 4. Downfield region of the ^{1}H NMR spectrum ($CDCl_3$, 400 MHz) of *c*,*c*,*c*-$RuCl_2$(dmso-S)(CO)(Me_3Bzm)$_2$ (**5**) (top) and *t*,*c*,*c*-$RuCl_2$(dmso-S)(CO)(Me_3Bzm)$_2$ (**6**) (bottom); resonances of Me_3Bzm "a" and "b" are labeled with a and b, respectively

a clear NOE cross-peak between the B4H resonance at δ = 7.96 and the dmso peak at δ = 3.11, it could be established that the two ligands are *cis* to one another. The overall chemical shift patterns of the Me_3Bzm "a" and "b" ligands in **5** closely resemble those found in the HH rotamer of *c*,*c*,*c*-$RuCl_2$(dmso-S)$_2$(Me_3Bzm)$_2$ (**1**-HH, Table 4); in particular, the (B4H)b and ($B10H_3$)b signals are upfield shifted, suggesting that these protons might reside within the shielding cone of Me_3Bzm "a". Similarly, the upfield shift of the (B2H)a signal and, to a lesser extent, that due to ($B12H_3$)a, can be attributed to their positions within the shielding cone of Me_3Bzm "b". According to such arguments, an HH conformation similar to that found in the crystal structure of **5** (see below and Table 3) is most likely maintained in solution.

of B4H, is maintained. It might be argued that such differences are caused by the presence of CO instead of dmso-S in the coordination sphere of the ruthenium center. However, the Me_3Bzm chemical shifts are very similar in the corresponding mono-Me_3Bzm derivatives, *c*,*c*,*c*-$RuCl_2$(dmso-S)$_2$(CO)(Me_3Bzm) and *cis*,*fac*-$RuCl_2$(dmso-S)$_3$(Me_3Bzm), which differ only in the presence of a CO molecule in place of a dmso-S ligand in position "a".[12] This finding suggests that the differences in Me_3Bzm chemical shifts found between **1**-HH and **5** are not due to the different ligand environments (CO vs. dmso-S), but rather to a slightly different average mutual tilt between the two HH ligands in solution.[1]

The ambient-temperature NMR spectrum of **5**, which shows only one set of resonances, is consistent with two hypotheses: either both the Me_3Bzm ligands are in rapid motion about the Ru−N bonds, averaging the HH conformation, or they both remain in relatively fixed positions. Variable-temperature NMR spectra of **5** in CD_2Cl_2 showed a partial broadening of the peaks only at $T < -90$ °C, which is still compatible with both hypotheses (the very low temperature broadening might also be due to restricted motion of the sulfoxides).

cis,*cis*,*cis*-$RuCl_2(CO)_2(Me_3Bzm)_2$ (**7**)

Further formal replacement of the remaining dmso-S ligand in **5** by CO led to compound **7**, in which both positions "c" and "d" are occupied by CO ligands (Scheme 3). Overall, the Me_3Bzm resonances of **7** give rise to a pattern similar to that seen for **5** and typical of the HH orientation

Table 4. Chemical shifts (δ values) of *c*,*c*,*c*-$RuCl_2$(dmso-S)(CO)(Me_3Bzm)$_2$ (**5**), *t*,*c*,*c*-$RuCl_2$(dmso-S)(CO)(Me_3Bzm)$_2$ (**6**), and *c*,*c*,*c*-$RuCl_2(CO)_2(Me_3Bzm)_2$ (**7**) in $CDCl_3$ compared to those of the corresponding ligands in the HH conformer of *c*,*c*,*c*-$RuCl_2$(dmso-S)$_2$(Me_3Bzm)$_2$ (**1**)

	5		**6**		**7**		**1**[a]	
	Me_3Bzm "a"	Me_3Bzm "b"	Me_3Bzm "a"	Me_3Bzm "b"	Me_3Bzm "a"	Me_3Bzm "b"	Me_3Bzm "a"	Me_3Bzm "b"
B2H	8.15	8.56	8.67	7.55	7.82	8.83	7.43	8.90
B4H	7.96	6.24	7.50	8.14	7.63	6.16	8.25	6.11
B7H	7.14	7.07	7.14	7.11	7.19	7.17	7.06	7.17
$B10H_3$	2.44	1.86	2.05	2.39	2.52	1.90	2.48	1.85
$B11H_3$	2.43	2.26	2.31	2.40	2.46	2.30	2.41	2.31
$B12H_3$	3.56	3.78	3.82	3.55	3.57	3.88	3.36	3.92
	dmso-S "c"		dmso-S "c"				dmso-S "c"	
	3.55	3.11	3.41				3.55	2.86

[a] Conformer HH.

Despite the general similarity between the Me_3Bzm chemical shift patterns of **5** and **1**-HH, there are, nevertheless, some notable differences, particularly in the signal shifts of Me_3Bzm "a". Thus, while in **1**-HH the B4H signal appears further downfield than that of B2H, in **5** the "normal" order, i.e. the B2H signal further downfield than that (Table 4); the presence of CO in place of the residual dmso-S apparently has no significant effect on the resonances of the *trans*-coordinated Me_3Bzm. In this case, a NOESY spectrum did not allow us to distinguish between positions "a" and "b" and thus we assumed the HH orientation of the two Me_3Bzm ligands to be very similar to that in **5**.

However, a "reciprocal" HH orientation cannot be excluded (see below for **6**). From the point of view of the dynamics of the Me_3Bzm ligands, the ^1H NMR spectrum of **7** (which remained essentially unchanged in the temperature range +20 to −90 °C) is consistent with both the hypotheses advanced for **5**.

trans,cis,cis Compounds

trans,cis,cis-$RuCl_2$(dmso-S)$_2$(Me_3Bzm)$_2$ (**3**)

The room-temperature reaction of *trans*-$RuCl_2$(dmso-S)$_4$ with an excess of Me_3Bzm selectively yielded the bis-substituted adduct **3**, which is a geometrical isomer of *c,c,c*-$RuCl_2$(dmso-S)$_2$(Me_3Bzm)$_2$ (**1**) (Scheme 1). The NMR spectrum of **3** is very simple (one set of peaks due to the two equivalent Me_3Bzm ligands and one sharp resonance due to the four equivalent dmso-S methyl groups) and consistent with the C_{2v} symmetry of the complex (considering the ligands as point groups). This NMR spectral pattern indicates that at room temperature the two Me_3Bzm ligands are in rapid motion about the Ru−N bonds, most probably going from one HT conformation to the other, through the HH conformation. The variable-temperature behavior of the NMR spectrum of **3** (CD_2Cl_2) is rather complicated and scarcely informative; all resonances broaden as the temperature is lowered to below −20 °C, and at −60 °C two sets of peaks in an almost 1:2 ratio begin to appear. However, on decreasing the temperature further, some of the signals broaden once more. These findings suggest that on lowering the temperature the rate of more than one molecular motion in **3** is sequentially decreased.

trans,cis,cis-$RuCl_2$(dmso-S)(CO)(Me_3Bzm)$_2$ (**6**)

The formal replacement of a dmso-S ligand in **3** by a CO ligand (Scheme 4) led to *trans,cis,cis*-$RuCl_2$(dmso-S)(CO)(Me_3Bzm)$_2$ (**6**), which is a geometrical isomer of **5** (Scheme 5). Compound **6**, while maintaining the overall geometry of **3**, nevertheless, has lower symmetry and thus provided useful spectroscopic information.

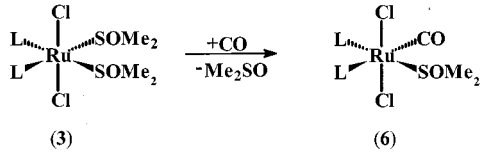

(3) (6)

Scheme 4

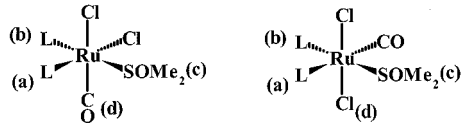

Scheme 5 (5) (6)

The NMR spectrum of **6** (Figure 4), in agreement with the geometry of the complex (confirmed by X-ray structure analysis, see below), consists of a set of resonances due to each non-equivalent Me_3Bzm ligand and a singlet due to the two enantiotopic methyl groups of the dmso-S ligand (δ = 3.41). This means that the N,N,S,C plane is a plane of symmetry for the complex and, as in **3**, the two Me_3Bzm ligands have averaged "side" (S) orientations. The signals were assigned with the aid of an NOESY spectrum (Table 4); an NOE cross-peak between the dmso-S and the B4H signal at δ = 8.14 allowed us to establish which of the Me_3Bzm ligands was *cis* to dmso-S. In **6**, the two *cis*-Me_3Bzm ligands and the dmso-S ligand have the same *mer* arrangement as in the geometrical isomer **5**, so that the same labeling scheme can be used (Scheme 5). Indeed, the NMR spectra of **6** and **5** are quite similar and both are in agreement with an HH orientation of the two bases. However, in **6** the chemical shift patterns of Me_3Bzm "a" and "b" are inverted with respect to those in **5** (Figure 4).

It might be argued that the different Me_3Bzm chemical shift patterns in **5** and **6** are due to the strong *trans* effect of the CO ligand. However, on the basis of results obtained for similar compounds,[13] substitution of dmso-S by CO is expected to affect the resonance of the proton closest to the N−Ru, i.e. B2H of Me_3Bzm "a", only marginally (ca. 0.3 ppm). The large chemical shift variations for the protons of Me_3Bzm "a" quite distant from the coordination site (e.g. $B10H_3$) and, above all, for the protons of Me_3Bzm "b" can thus safely be ascribed to a different mutual tilt of the two HH bases in **6** as compared to the situation in **5**. Indeed, in **6**, due to the lower symmetry compared to **3**, the two HH bases may either be leaning toward the dmso-S in position "c" or toward the CO (conformers H_2H_4 and H_1H_3 in Scheme 6, respectively; see Discussion). The NMR spectrum suggests that in solution the HH orientation of the two bases in **6** is such that (B4H)a and ($B10H_3$)a reside within the shielding cone of Me_3Bzm "b"; models show that this is accomplished when the two HH bases are inclined toward the dmso-S (conformer H_2H_4). This orientation, which is the opposite to that found in **1** and **5**, is also evident in the solid-state structure (Figure 3, Table 3).

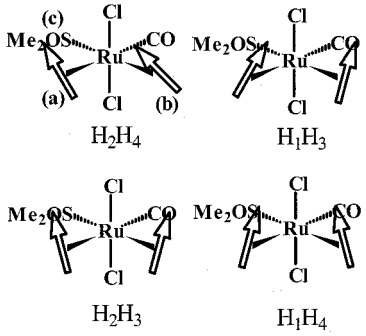

Scheme 6

Variable-temperature NMR experiments in CD_2Cl_2 showed that the resonances of the two bases in **6** begin to broaden only at temperatures below −80 °C, while at such temperatures the dmso-S resonance splits into two equally intense peaks (δ = 3.35 and 3.31). This behavior suggests that at room temperature the two HH bases are most probably in rapid motion between two equivalent HH orientations, one above and the other below the N,N,S,C plane, thus averaging out as an "S" orientation. These motions

might be accompanied by that of dmso-S [so that the electrostatic interaction between (B2H)a and the oxygen atom of dmso is maintained]. At very low temperature (−80 °C), these motions (or those of the dmso-S ligand) become slow on the NMR time scale, the N,N,S,C pseudo-symmetry plane is lost, and the two methyl groups of the dmso-S become diastereotopic.

Discussion

Conformational Definitions

In unsymmetrical octahedral complexes of the type *c*,*c*,*c*-$RuCl_2(X)(Y)(Me_3Bzm)_2$, where X, Y = dmso-S or CO, two HH and two HT diastereotopomers are possible. Thus, it is necessary to designate the possible HH and HT geometries. In fact, taking the chlorine atom *cis* to both N ligands as a reference, quite different environments are achieved if the head of the Me_3Bzm ligand (B2H) is directed toward this chlorine atom or points in the opposite direction. We will indicate these positions as "up" (u) and "down" (d), respectively, so that the two HH geometries will be labeled as $(HH)_u$ and $(HH)_d$ (Scheme 2). For a more precise description of the HT conformations, the orientation of one of the two bases must be selected; we shall assume that the "u" and "d" descriptors in $(HT)_u$ and $(HT)_d$ always refer to the head of ligand "a". Furthermore, for a complete stereochemical description of such complexes, we reiterate that they can exist as enantiomeric pairs, the chirality of which can be described as Δ and Λ, taking the N···N and Cl···Cl vectors as skew lines.[14] The schemes and Figures 1−3 depict Δ enantiomers.

In order to study hindered rotation about the Ru−N bonds, torsion angles must be introduced, such as $\Psi_a = N_b-Ru-N_a-C_{\alpha a}$ and $\Psi_b = N_a-Ru-N_b-C_{\alpha b}$, where the subscripts a and b refer to the two nitrogen bases and C_α is the carbon atom in position 2 (Scheme 1). These parameters provide a precise description of all the possible HH and HT conformations, and also allow a distinction to be made between the different "head" orientations (see below). In the case of the enantiomorph Δ, $-180° < \Psi_a < 0°$ and $0° < \Psi_b < 180°$ for $(HH)_u$, and $0° < \Psi_a < 180°$, $-180° < \Psi_b < 0°$ for $(HH)_d$. The angular relationships between $(HH)_u$ and $(HH)_d$ are interchanged for the enantiomorph Λ. For the isomers $(HT)_u$ and $(HT)_d$, the ranges for the torsion angles are $-180° < \Psi_{a,b} < 0°$ and $0° < \Psi_{a,b} < 180°$, respectively. The Ψ angles also provide a quantitative measure of the mutual tilt of the two bases, which vanishes only when $\Psi_a = \Psi_b = \pm 90°$. If $\Psi = 0°$ or 180°, the hypothetical side (S) orientation occurs.

However, the (u) and (d) descriptors alone cannot adequately describe all the possible HH and HT conformations. For example, in the case of *t*,*c*,*c*-$RuCl_2(X)(Y)(Me_3Bzm)_2$ complexes there are no enantiomorphs, and the distinction between the "up" and "down" conformers is meaningless. Obviously, when X = Y, positions "a" and "b" are interchangeable; however, when X = CO and Y = dmso-S, as in *t*,*c*,*c*-$RuCl_2$(dmso-S)(CO)$(Me_3Bzm)_2$ (**6**), the two Me_3Bzm ligands are no longer equivalent, and substantially different HH and HT geometries are possible (see Scheme 6 with four HH conformers in **6**). The same concept also applies to *cis*,*cis*,*cis* complexes in which, for each $(HH)_{u/d}$ and $(HT)_{u/d}$ conformation, the two lopsided bases can have a range of different reciprocal orientations.

On the basis of the Ψ values, it is possible to formulate a new descriptor, such as $H_{\Psi a}H_{\Psi b}$ (head Ψ_a−head Ψ_b), to represent the mutual orientation of two *cis* lopsided ligands. For a simpler representation, we can use the notation H_iH_j (head *i*−head *j*), where *i* and *j* refer to the quadrants of Ψ_a and Ψ_b, respectively (*i*, *j* = 1: $0° < \Psi < 90°$; *i*, *j* = 2: $90° < \Psi < 180°$; *i*, *j* = 3: $180° < \Psi < 270°$; *i*, *j* = 4: $270° < \Psi < 360°$). This provides a simple means of describing in detail each HH and HT conformation; for example, the four HH conformers depicted in Scheme 6 can be described as H_2H_4, H_1H_3, H_2H_3, and H_1H_4, respectively. The system is particularly convenient when the torsion angles are around ±45° (or supplementary values), as found for lopsided aromatic bases.

The inter-base dihedral angle (Φ) has often been used to describe the conformations of metal complexes containing *cis* nitrogen bases.[15−17] This parameter, however, is of limited scope since, as is clear from the data in Table 3, different orientations (HH and HT) may have almost identical Φ values.

In *cis*,*cis*,*cis* complexes, when X = Y = dmso-S, the same conformational descriptors defined above for Me_3Bzm can be used for the two *cis*-dmso ligands, considering the position of the sulfoxide oxygen atom (taken as the head of the ligand) with respect to the RuS_2 plane and of the chlorine atom *cis* to both dmso ligands. If the oxygen atom lies in the RuS_2 plane, it is in a "planar" (P) orientation. Rotation about the Ru−S bonds is described by the torsion angles $\Psi_c = O_c-S_c-Ru-S_d$ and $\Psi_d = O_d-S_d-Ru-S_c$. In the case of the Δ enantiomorph, $0° < \Psi_c < 180°$, $-180° < \Psi_d < 0°$ and $-180° < \Psi_c < 0°$, $0° < \Psi_d < 180°$, for $(HH)_u$ and $(HH)_d$, respectively. For the $(HT)_u$ and $(HT)_d$ isomers (descriptors u and d being referred to the head of ligand "c"), the ranges of both the torsion angles, Ψ (= Ψ_c, Ψ_d), are: $0° < \Psi < 180°$ for $(HT)_u$ and $-180° < \Psi < 0°$ for $(HT)_d$. However, when the torsion angles are close (±15°) to the limiting values of 0°, 90°, 180°, and 270°, as for Ψ_c and Ψ_d in *cis*-sulfoxides, the more general descriptor $H_{\Psi c}H_{\Psi d}$ would seem to be more appropriate, e.g. $H_0H_{\pi/2}$ and H_0H_π, when $\Psi_c = 0°$ and $\Psi_d = 90°$ and 180°, respectively (see Table 3).

Molecular Conformations

It is interesting (cf. Table 3) that all the Δ *c*,*c*,*c*-RuX_2(dmso-S)$_2(Me_3Bzm)_2$ derivatives display HH geometries (more precisely, H_4H_2) for the Me_3Bzm ligands in the solid state, irrespective of the nature of X (Cl or Br) or of their different packing and van der Waals interactions with polar (ethanol, **2**; methanol, **5**) or apolar (benzene, **8**) solvent molecules of crystallization. However, in solution they all undergo equilibration with HT isomers of comparable stability (Table 5). It is thus clear that intermolecular pack-

Table 5. Rotamer distribution in solution and calculated relative strain energy ratios for *c*,*c*,*c*-$RuX_2(dmso\text{-}S)_{2-n}(CO)_n(L1)(L2)$ complexes, with X = Cl, Br; n = 0, 1; L1, L2 = Me_3Bzm, Me_2Im

Complex	Rotamers	Population ratios	Relative strain energy ratios
c,*c*,*c*-$RuCl_2(dmso\text{-}S)_2(Me_3Bzm)_2$	HH, HT[a]	1:0.8[a]	2.1:0[b]
c,*c*,*c*-$RuBr_2(dmso\text{-}S)_2(Me_3Bzm)_2$	HH, HT[a]	1:0.8[a]	
c,*c*,*c*-$RuCl_2(dmso\text{-}S)_2(1,2\text{-}Me_2Im)(Me_3Bzm)$	HH, HT[c]	1:5.0[c]	1.1:0[b]
c,*c*,*c*-$RuCl_2(dmso\text{-}S)_2(1,2\text{-}Me_2Im)_2$	HT, HH, HT, HH[c]	1.5:3.4:1.5:1[c]	0.6:0:0.9:1.3[d]
c,*c*,*c*-$RuCl_2(dmso\text{-}S)(CO)(Me_3Bzm)_2$	HH, HT[b]	1.0:0[b]	0:0.2[b]

[a] Ref.[3] – [b] Present work. – [c] Ref.[4] – [d] Ref.[18a]

ing forces are responsible for the exclusive crystallization of one form. From Table 3, it is evident that the formal substitution of a Me_3Bzm ligand by 1,2-Me_2Im (which occurs only at position "a") causes a stabilization of the HT geometry in the solid state, which is partially maintained in solution (Table 5).[4] Interestingly, in the case of *c*,*c*,*c*-$RuCl_2(dmso\text{-}S)_2(1,2\text{-}Me_2Im)(3,5\text{-lut})$, two rotamers (R1, R2) with opposite orientations of the 1,2-Me_2Im ligand were found to be present in the same crystal (ratio 0.63:0.37) as well as in solution (ratio 0.7:0.3).[5] Overall, the results indicate that the nature and relative abundance of the rotamers in solution depends markedly on the nature of the nitrogen bases; in the solid state, the equilibrium position can easily be shifted from the solution position by crystal packing effects that stabilize only one of the conformers. Generally, as shown by MM calculations,[18] the solid-state geometry corresponds to the lowest strain energy structure.

As already mentioned, it has been postulated that the hindered rotation of Me_3Bzm "b" in *c*,*c*,*c*-$RuCl_2(dmso\text{-}S)_2(Me_3Bzm)_2$ (**1**) arises from the electrostatic attraction between its acidic B2H proton and the negatively charged Cl ligands.[1] This hypothesis is supported by the present MM calculations. In fact, in the two lowest-energy conformers of Δ **1**, $(HT)_d$ and $(HH)_u$, (Table 6), Ψ_b is always about 135.6°, well within the range of 131.5−138.1° found in the solid state (Table 3). In both cases, rotation of 180° about the Ru−N_b bond ($\Psi_b \approx -44°$) causes a significant increase in the molecular strain energy [4.4 kcal mol^{-1} $(HT)_d \rightarrow (HH)_d$; 4.0 kcal mol^{-1} $(HH)_u \rightarrow (HT)_u$]; about 3 kcal mol^{-1} of this increase can be attributed to a decrease in the attractive electrostatic term (Table 6).

The favorable features of this orientation for Me_3Bzm "b" are further shown by the results relating to *c*,*c*,*c*-$RuCl_2(dmso\text{-}S)_2(1,2\text{-}Me_2Im)(Me_3Bzm)$, for which only the $(HT)_d$ (namely H_2H_2) conformer is present in the solid state and also predominates in solution (Table 5). MM calculations are in agreement with this observation, the energy of the $(HT)_d$ conformer being 1.1 kcal mol^{-1} lower than that of the $(HH)_u$ form (Table 7).

Another important result of this work is the observation that in all the Δ *c*,*c*,*c*-$RuCl_2(dmso\text{-}S)_2(L1)(L2)$ compounds in Table 3, the dmso conformation is invariably $(HH)_d$, with average values for Ψ_c and Ψ_d of $-14 \pm 12°$ and $86 \pm 6°$, respectively. This conformation corresponds to structures in which the O atom of each dmso lies approximately in the coordination plane perpendicular to the Ru−S bond of the other dmso, with the methyl groups of each dmso straddling a Ru−Cl bond. Similar conformations are found in all the minimum-energy structures calculated for the $(Me_3Bzm)_2$ and $(1,2\text{-}Me_2Im)(Me_3Bzm)$ derivatives (Tables 6 and 7). When this conformation is changed, there is a marked increase in the strain energy (Table 7). Interestingly, NMR data suggest that this geometry of the *cis*,*cis*-$RuCl_2(dmso\text{-}S)_2$ fragment is also predominant in solution.[5] In **5**, the presence of a CO group in "d" induces a rotation of ca. 80° about the Ru−S bond for dmso-S "c" (dmso O atom in the coordination plane and methyl groups again straddling a Ru−Cl bond), showing that the interligand steric interactions play a crucial role in determining the dmso orientation. Furthermore, density functional calculations on Ru^{II}(dmso-S) model molecules have shown that, even in the case of significant π bonding, steric factors far outweigh electronic effects.[19]

For *t*,*c*,*c*-$RuCl_2(dmso\text{-}S)_2(Me_3Bzm)_2$ (**3**), in agreement with the solution NMR data, MM results show (Table 8) that molecules with HT and HH base conformations have almost the same energy (max. difference 0.32 kcal mol^{-1}). Each conformer can adopt two structures with very similar minimum energies, differing only in the dmso orientation. Similar results have been obtained for *t*,*c*,*c*-$RuCl_2(dmso\text{-}S)_2(Bzm)_2$ (**4**) (Table 9). In both cases, crystallization stabilizes the HH geometry (Table 3). In solution, in agreement with NMR results, quick flipping between the isoenergetic

Table 6. Total strain energy E [kcal mol^{-1}] with the stretching (E_s), bending (E_b), torsional (E_t), van der Waals (E_v), and electrostatic (E_e) contributions [kcal mol^{-1}] for the four lowest-energy diastereotopomers of Δ *c*,*c*,*c*-$RuCl_2(dmso\text{-}S)_2(Me_3Bzm)_2$; torsion angles Ψ [°] with the base and dmso conformation descriptors are also given

E	Ψ_a	Ψ_b	base		Ψ_c	Ψ_d	dmso		E_s	E_b	E_t	E_v	E_e
3.87	135.5	135.9	$(HT)_d$	H_2H_2	−30.5	88.1	$(HH)_d$	H_4H_1	2.47	45.6	0.28	−3.09	−41.4
6.03	−45.9	135.4	$(HH)_u$	H_4H_2	−16.2	95.5	$(HH)_d$	H_4H_2	2.48	47.0	0.06	−1.87	−41.6
8.31	132.3	−42.6	$(HH)_d$	H_2H_4	−30.4	105.4	$(HH)_d$	H_4H_2	2.55	45.6	0.07	−1.45	−38.4
10.0	−53.0	−46.6	$(HT)_u$	H_4H_4	−22.2	109.1	$(HH)_d$	H_4H_2	2.60	46.8	0.02	−0.72	−38.7

Table 7. Total strain energy E [kcal mol^{-1}] with the stretching (E_s), bending (E_b), torsional (E_t), van der Waals (E_v), and electrostatic (E_e) contributions [kcal mol^{-1}] for the four lowest-energy diastereotopomers of Δ *c*,*c*,*c*-$RuCl_2$(dmso-S)$_2$(1,2-Me_2Im)(Me_3Bzm); torsion angles Ψ [°] with the base and dmso conformation descriptors are also given

E	Ψ_a	Ψ_b	base		Ψ_c	Ψ_d	dmso		E_s	E_b	E_t	E_v	E_e
6.18	132.1	136.9	$(HT)_d$	H_2H_2	−26.9	91.7	$(HH)_d$	H_4H_2	2.12	44.0	3.56	−2.90	−40.6
7.28	−40.7	135.3	$(HH)_u$	H_4H_2	−20.9	99.1	$(HH)_d$	H_4H_2	2.15	45.2	3.59	−2.31	−41.4
9.93	127.2	−43.4	$(HH)_d$	H_2H_4	−29.9	109.7	$(HH)_d$	H_4H_2	2.18	43.9	3.50	−1.75	−37.9
11.1	135.1	140.1	$(HT)_d$	H_2H_2	−28.7	−169.4	$(HT)_d$	H_4H_3	2.45	45.6	3.77	−2.45	−38.3

HH and HT geometries may be envisaged, to give an average side orientation.

Table 8. Total strain energy E [kcal mol^{-1}] with the stretching (E_s), bending (E_b), torsional (E_t), van der Waals (E_v), and electrostatic (E_e) contributions [kcal mol^{-1}] for the four lowest-energy diastereotopomers of *t*,*c*,*c*-$RuCl_2$(dmso-S)$_2$(Me_3Bzm)$_2$; torsion angles Ψ [°] with the base and dmso conformation descriptors are also given

E	Ψ_a	Ψ_b	base	Ψ_c	Ψ_d	dmso	E_s	E_b	E_t	E_v	E_e
11.34	130.5	125.2	HT	24.3	168.8	HT	2.57	46.1	0.55	−2.35	−35.5
11.45	129.4	124.8	HT	8.7	−178.1	PP[a]	2.66	46.3	0.61	−0.94	−37.2
11.48	−57.2	130.0	HH	22.7	168.7	HT	2.63	46.8	0.15	−0.83	−37.2
11.66	−57.2	129.0	HH	20.0	178.0	HT	2.71	46.9	0.18	0.01	−38.1

[a] Both oxygen atoms in the Ru−S_2 plane.

Table 9. Total strain energy E [kcal mol^{-1}] with the stretching (E_s), bending (E_b), torsional (E_t), van der Waals (E_v), and electrostatic (E_e) contributions [kcal mol^{-1}] for the four lowest-energy diastereotopomers of *t*,*c*,*c*-$RuCl_2$(dmso-S)$_2$(Bzm)$_2$; torsion angles Ψ [°] with the base and dmso conformation descriptors are also given

E	Ψ_a	Ψ_b	base	Ψ_c	Ψ_d	dmso	E_s	E_b	E_t	E_v	E_e
8.24	130.4	125.3	HT	24.2	168.8	HT	1.98	44.9	0.26	−0.93	−38.0
8.36	129.5	125.0	HT	9.3	−178.4	PP	2.07	45.3	0.29	0.45	−39.7
8.43	129.5	−58.0	HH	22.9	168.7	HT	2.05	45.6	0.06	0.21	−39.5
8.60	128.7	−57.5	HH	21.5	177.3	HT	2.13	45.8	0.08	0.99	−40.4

Unlike in the *cis*,*cis*,*cis* compounds, the solid-state conformation of the dmso groups in the *trans*,*cis*,*cis* compounds (**3** and **4**) is HT, with Ψ values of about 31° and 161° (Table 3). These values are close to the minimum energy structure values of about 24° and 169° (Tables 8 and 9). In this conformation, the two oxygen atoms are significantly displaced from the Ru−S_2 plane (ca. ±0.45 Å). However, MM calculations indicate that the energy difference between these HT arrangements and the PP arrangement (both oxygen atoms in the Ru−S_2 plane) is very small (ca. 0.1 kcal mol^{-1}) (Tables 8 and 9). In fact, a strictly symmetry-determined PP geometry of pairs of *cis*-sulfoxide ligands has been observed in *trans*-RuX_2(dmso-S)$_4$ complexes (X = Cl, Br).[20]

As in the case of **5**, substitution of one dmso group in **6** by CO causes a significant rotation about the Ru−S bond of the remaining dmso (Ψ_c approximately from 32° to −109°, Table 3). Most interestingly, the HH base mutual orientation in **6** is opposite to that found in **3** (as well as **1** and **5**), as shown by the Ψ_a and Ψ_b values (Table 3 and Figure 3). In fact, the base orientation in **3** is H_4H_2, while in **6** it is H_2H_4, as also found in solution. Such an arrangement of the neutral ligands brings the positively charged B2H of base "a" close to the negatively charged oxygen atom of dmso (H···O 3.0 Å) and to one chloride ligand (H···Cl 2.9 Å).

Limitations and Prospects for the MM Force Field

As discussed above, the force field used in the present MM calculations can describe the lowest strain energy structures in good agreement with those found in the solid state. The force field has also been found to be adequate for studying the possible rotamer distributions in solution for Ru^{II}(dimethyl sulfoxide) complexes containing lopsided nitrogen ligands such as 3,5-lutidine and 1,2-dimethylimidazole.[18a] However, inspection of the data in Table 5 shows that, unlike for the other derivatives, for *c*,*c*,*c*-$RuCl_2$(dmso-S)$_2$(Me_3Bzm)$_2$ (**1**) the strain energy ratio is not in agreement with the solution NMR data, which show that the HH and HT diastereotopomers are present in an approximately equimolar ratio. In fact, according to the MM results (Table 6), the diastereotopomer $(HT)_d$ should be predominant with a strain energy 2.1 kcal mol^{-1} lower than that of $(HH)_u$ due to a more negative contribution of the van der Waals term. It seems likely that this "anomalous" solution behavior observed in the case of *cis*-Me_3Bzm ligands is related to the larger surface area of Me_3Bzm compared to smaller ligands such as 1,2-Me_2Im and the consequently stronger interactions with solvent molecules. In fact, in solution, the two isomers of **1** are present in an almost 1:1 ratio, but only one form is present in the solid state, showing the importance of the packing intermolecular interactions. The "failure" of the MM calculations to give the lowest energy topomer in solution for **1** should be mainly due to the neglection of the effects of solvent interactions. The solvent-accessible surface area (SA) for *c*,*c*,*c*-$RuCl_2$(dmso-S)$_2$(Me_3Bzm)$_2$ is 738.7 Å^2 for the HH diastereoisomer and 718.2 Å^2 for the HT form, while it amounts to 720.7 and 705.6 Å^2, respectively, for the HH and HT isomers of *c*,*c*,*c*-$RuCl_2$(dmso-S)(CO)(Me_3Bzm)$_2$ (**5**). The greater SA values for the HH geometries could allow for more effective interactions with the solvent molecules, thereby stabilizing these forms in solution.

In any case, it must be kept in mind that the force field constants used in this work have been optimized only on the basis of crystal structure data.[18a] No thermodynamically observable parameter has been introduced, hence the calculated energy differences must be considered with caution. Another limitation of the present MM method re-

lates to the evaluation of energy barriers for rotation about the Ru−N bonds. These barriers are probably overestimated owing to the inability of the force field to describe non-minimum-energy structures. For this, non-harmonic functions and correlation terms would need to be introduced. Thus, the energy barrier of about 17 kcal mol^{-1} calculated for rotation about the Ru−N bonds in **1** must be considered merely as an indication of hindered rotation. On the other hand, a similar energy barrier of about 16 kcal mol^{-1} has been calculated for the *trans* compound **3**, for which fast rotation about the Ru−N bonds has been found in solution, showing the limited meaning of these values.

Conclusions

We have investigated the factors that influence the relative orientation and dynamic motion of the *cis*-Ru$(Me_3Bzm)_2$ unit in Ru^{II}(dimethyl sulfoxide) compounds of the general formula $RuCl_2(dmso\text{-}S)_{2-n}(CO)_n(Me_3Bzm)_2$ ($n = 0-2$). Complexes with *cis* and *trans* arrangements of the Cl ligands have been prepared and structurally characterized both in solution and in the solid state by NMR and X-ray techniques, respectively. The results have been compared with those obtained previously with the thoroughly studied *c*,*c*,*c*-$RuCl_2(dmso\text{-}S)_2(Me_3Bzm)_2$ (**1**). The influences of the nature of the halide ligands (Br vs. Cl) and of the medium of crystallization on the solid-state conformation of **1** have been also investigated. The experimental molecular conformations have been discussed on the basis of molecular mechanics (MM) calculations.

While for **1** two almost equally populated ligand orientations (HH and HT) are found in solution, replacement of one or both dmso-S molecules by CO ligands leads to the complexes *c*,*c*,*c*-$RuCl_2(dmso\text{-}S)(CO)(Me_3Bzm)_2$ (**5**) and *c*,*c*,*c*-$RuCl_2(CO)_2(Me_3Bzm)_2$ (**7**), respectively, for which only one HH orientation is preferentially populated in solution. It remains unclear as to whether in such conformers rotation of the bases about the Ru−N bonds is slow or very fast on the NMR time scale; in other words, the torsional barriers have not been estimated. Only the HH orientation was found in the solid-state structure of **5**.

We have found that the two *cis*-Me_3Bzm bases also maintain a preferential HH orientation when the geometry of the Cl ligands is changed from *cis* to *trans*; the preference for such an orientation has been demonstrated in solution for *t*,*c*,*c*-$RuCl_2(dmso\text{-}S)(CO)(Me_3Bzm)_2$ (**6**) and in the solid state for both **6** and *t*,*c*,*c*-$RuCl_2(dmso\text{-}S)_2(Me_3Bzm)_2$ (**3**). In the corresponding benzimidazole (Bzm) compound, *t*,*c*,*c*-$RuCl_2(dmso\text{-}S)_2(Bzm)_2$ (**4**), the two bases are also HH disposed in the solid state. In solution at ambient temperature, NMR evidence indicates that the two *t*,*c*,*c* complexes **3** and **6** behave differently. Thus, while the two *cis*-Me_3Bzm ligands are in rapid motion about the Ru−N bonds in **3**, most probably going from one HT conformation to the other through the HH conformation, in **6** the two bases are seemingly in rapid motion between two equivalent HH orientations, one above and the other below the N,N,S,C plane, thus averaging out as an "S" orientation. Moreover, both in solution and in the solid state, the mutual tilt of the HH bases in **6** is the opposite to that found in **1** and **5**.

Electrostatic interaction between the halide ligands and the positively charged N_2CH proton on the imidazole ring has been found to be the essential factor in determining the specific orientation of one Me_3Bzm base, both in the solid state and in solution. Comparison of the solid-state and solution structures with those predicted by MM calculations has revealed that intermolecular interactions can play a significant role in determining the orientation of the second Me_3Bzm ligand.

Experimental Section

Reagents: Analytical-grade solvents were used without further purification. All reagents, including CD_2Cl_2 and $CDCl_3$, were purchased from Aldrich.

Starting Materials: *cis*-$RuCl_2(dmso)_4$,[20] *trans*-$RuCl_2(dmso\text{-}S)_4$,[20] *cis*,*fac*-$RuCl_2(dmso)_3(CO)$,[11] *trans*-$RuCl_2(dmso)_3(CO)$,[11] *c*,*c*,*c*-$RuCl_2(dmso)_2(CO)_2$,[11] *c*,*c*,*c*-$RuCl_2(dmso\text{-}S)_2(Me_3Bzm)_2$ (**1**),[3] *c*,*c*,*c*-$RuBr_2(dmso\text{-}S)_2(Me_3Bzm)_2$ (**2**),[3] and *t*,*c*,*c*-$RuCl_2(dmso\text{-}S)_2(Bzm)_2$ (**4**)[21] were prepared by known methods.

***trans*,*cis*,*cis*-$RuCl_2(dmso\text{-}S)_2(Me_3Bzm)_2$ (3):** The complex was synthesized using as starting material either *cis*-$RuCl_2(dmso)_4$ (path a) or, preferably, *trans*-$RuCl_2(dmso\text{-}S)_4$ (path b): (a) Me_3Bzm (0.36 g, 2.25 mmol) was added to a solution of *cis*-$RuCl_2(dmso)_4$ (0.5 g, 1 mmol) in chloroform (20 mL) and the reaction was allowed to proceed overnight at room temperature. The mixture was then concentrated in vacuo to a volume of ca. 5 mL, diethyl ether (5 mL) was added dropwise, and the resulting solution was stored at 4 °C. Deep-yellow microcrystals of the product formed within 24 h, which were collected by filtration, washed with diethyl ether, and dried in vacuo. Yield 0.3 g (40%). The product was found to crystallize with one molecule of chloroform and is therefore better formulated as *t*,*c*,*c*-$RuCl_2(dmso\text{-}S)_2(Me_3Bzm)_2 \cdot CHCl_3$. Further concentration of the mother liquor yielded a second crop of precipitate. However, ^1H NMR analysis showed this to be a mixture of **3** and the *c*,*c*,*c* isomer **1**. − (b) *trans*-$RuCl_2(dmso\text{-}S)_4$ was treated with Me_3Bzm under the same conditions as used for the *cis* isomer in procedure (a). In this case, the yield was higher (70%) and no evidence for formation of the corresponding *c*,*c*,*c* isomer **1** was found. − Recrystallization from CH_2Cl_2/dmso mixtures (50:1) and subsequent addition of diethyl ether yielded crystals suitable for X-ray analysis (yield 70%). − $C_{24}H_{36}Cl_2N_4O_2RuS_2$ (648.6): calcd. C 44.4, H 5.59, N 8.63, S 9.88; found C 44.4, H 5.54, N 8.58, S 9.98. − ^1H NMR ($CDCl_3$): δ = 2.19 (s, 6 H, $B11H_3$), 2.32 (s, 6 H, $B10H_3$), 3.33 (s, 12 H, dmso-S), 3.63 (s, 6 H, $B12H_3$), 7.06 (s, 2 H, B7H), 8.18 (s, 2 H, B4H), 8.34 (s, 2 H, B2H).

***cis*,*cis*,*cis*-$RuCl_2(dmso\text{-}S)(CO)(Me_3Bzm)_2$ (5):** *cis*,*fac*-$RuCl_2(dmso)_3(CO)$ (0.19 g, 0.44 mmol) was partially dissolved in toluene (12 mL). Me_3Bzm (0.21 g, 1.31 mmol) was added and the resulting mixture was heated to reflux. A clear, pale-yellow solution was obtained within 30 min and then a precipitate of the same color formed. After 1.5 h, the hot mixture was filtered, and the collected

solid was washed with cold toluene and diethyl ether and dried in vacuo at room temperature (yield 50%). ^{1}H NMR analysis showed the crude product to contain up to 20% *t*,*c*,*c*-$RuCl_2$(dmso-S)(CO)(Me_3Bzm)$_2$ (**6**). Pure **5** (according to NMR) was obtained by recrystallization of this crude product from acetone/dmso mixtures (0.25 g in 5 mL of acetone and 0.1 mL of dmso) and subsequent careful addition of diethyl ether at room temperature (yield 75%). − $C_{23}H_{30}Cl_2N_4O_2RuS$ (598.5): calcd. C 46.1, H 5.05, N 9.36; found C 46.2, H 5.06, N 9.46. − Crystals of **5** suitable for X-ray analysis were obtained by recrystallization from methanol.

***trans*,*cis*,*cis*-$RuCl_2$(dmso-S)(CO)(Me_3Bzm)$_2$ (6):** *trans*-$RuCl_2$-(dmso)$_3$(CO) (0.20 g, 0.46 mmol) was dissolved in methanol (16 mL) and Me_3Bzm (0.18 g, 1.15 mmol) was added. The reaction was allowed to proceed for 24 h at room temperature and then the mixture was concentrated to half of its original volume. A yellow, microcrystalline product precipitated within 24 h, which was collected by filtration, washed with cold methanol and diethyl ether, and dried in vacuo at room temperature (yield 80%). Crystals suitable for X-ray analysis were obtained upon slow diffusion of *n*-hexane into a chloroform solution of the complex. −

Table 10. Crystallographic data and refinement details for compounds **2**−**6** and **8**

	2·0.5 C_2H_5OH	**3**	**4**
Empirical formula	$C_{25}H_{39}Br_2N_4O_{2.5}RuS_2$	$C_{24}H_{36}Cl_2N_4O_2RuS_2$	$C_{18}H_{24}Cl_2N_4O_2RuS_2$
M_r	760.61	648.66	564.50
Crystal system	triclinic	monoclinic	orthorhombic
Space group	$P\bar{1}$	$P2_1/c$	*Pbca*
a [Å]	11.574(1)	15.290(3)	27.332(6)
b [Å]	11.730(2)	10.625(2)	11.599(1)
c [Å]	12.395(4)	17.933(2)	14.517(3)
α [°]	99.55(2)		
β [°]	89.87(2)	94.51(1)	
γ [°]	103.62(2)		
V [Å^3]	1611.6(6)	2904.3(9)	4602.2(14)
Z	2	4	8
$D_{calcd.}$ [mg m^{-3}]	1.567	1.483	1.629
μ(Mo-K_α) [mm^{-1}]	3.124	0.895	1.117
F(000)	766	1336	2288
θ limits [°]	2.24−27.97	2.23−27.96	2.30−29.96
Index ranges	$-15 \le h \le 15$	$-20 \le h \le 20$	$0 \le h \le 38$
	$-15 \le k \le 15$	$0 \le k \le 14$	$0 \le k \le 16$
	$0 \le l \le 16$	$0 \le l \le 23$	$0 \le l \le 20$
Data collected	8132	7581	7397
Unique data (R_{int})	7777 (0.025)	6951 (0.019)	7397
Observed reflections [$I > 2\sigma(I)$]	4831	4686	4391[a]
Parameters	353	326	266
Goodness-of-fit, *S*	1.174	1.144	1.067
*R*1, *wR*2 [$I > 2\sigma(I)$][b]	0.0480, 0.1112	0.0302, 0.0671	0.0349, 0.0896
*R*1, *wR*2 (all data)[b]	0.1278, 0.1688	0.0810, 0.0914	[a]
Residuals [e·Å^{-3}]	1.018, −0.790	0.498. −0.670	0.679, −0.689

	5·0.5 CH_3OH	**6**·0.5 CH_3OH	**8**·2 C_6H_6
Empirical formula	$C_{23.5}H_{32}Cl_2N_4O_{2.5}RuS$	$C_{23}H_{30}Cl_2N_4O_2RuS$	$C_{36}H_{48}Cl_2N_4O_2RuS_2$
M_r	614.56	598.5	804.87
Crystal system	triclinic	triclinic	monoclinic
Space group	$P\bar{1}$	$P\bar{1}$	$P2_1/c$
a [Å]	8.2245(7)	9.019(1)	13.790(2)
b [Å]	10.984(1)	10.879(1)	13.505(3)
c [Å]	16.036(2)	15.801(2)	21.410(5)
α [°]	106.81(1)	74.52(1)	
β [°]	98.37(1)	76.07(1)	97.36(2)
γ [°]	94.96(1)	75.08(1)	
V [Å^3]	1359.2(3)	1418.9(3)	3954.4(14)
Z	2	2	4
D_{calcd} [mg m^{-3}]	1.502	1.438	1.352
μ(Mo-K_α) [mm^{-1}]	0.880	0.843	0.672
F(000)	630	630	1672
θ limits [°]	2.01−27.97	2.15−26.99	2.12−27.98
Index ranges	$-10 \le h \le 10$	$-11 \le h \le 11$	$-18 \le h \le 18$
	$-14 \le k \le 14$	$-13 \le k \le 13$	$0 \le k \le 17$
	$0 \le l \le 21$	$0 \le l \le 20$	$0 \le l \le 28$
Data collected	6772	6464	10186
Unique data (R_{int})	6542 (0.027)	6179 (0.019)	9528 (0.095)
Observed reflections [$I > 2\sigma(I)$]	5390	4922	6612
Parameters	377	324	434
Goodness-of-fit, *S*	1.050	1.088	1.142
*R*1, *wR*2 [$I > 2\sigma(I)$][b]	0.0488, 0.1497	0.0420, 0.1234	0.0369, 0.0741
*R*1, *wR*2 (all data)[b]	0.0764, 0.2345	0.0566, 0.1303	0.0795, 0.0951
Residuals [e Å^{-3}]	1.281, −1.268	0.987, −0.551	0.498, −0.430

[a] Only reflections with $I > 3\sigma(I)$ were used in the refinement. − [b] $R1 = \Sigma||F_o| - |F_c||/\Sigma|F_o|$, $wR2 = [\Sigma w(F_o^2 - F_c^2)^2/\Sigma w(F_o^2)^2]^{1/2}$.

$C_{23}H_{30}Cl_2N_4O_2RuS$ (598.5): calcd. C 46.1, H 5.05, N 9.36; found C 45.9, H 5.16, N 9.30.

***cis*,*cis*,*cis*-$RuCl_2(CO)_2(Me_3Bzm)_2$ (7):** *c*,*c*,*c*-$RuCl_2(CO)_2(dmso)_2$ (0.11 g, 0.28 mmol) was partially dissolved in ethanol (20 mL). Me_3Bzm (0.10 g, 0.62 mmol) was added and the resulting mixture was heated to reflux for 1.5 h. A clear, colorless solution was obtained within 10 min. On cooling, a white precipitate formed, which was collected by filtration, washed with cold ethanol and diethyl ether, and dried in vacuo at room temperature (yield 52 mg, 40%). ^1H NMR analysis showed this precipitate to consist of *c*,*c*,*t*-$RuCl_2(CO)_2(Me_3Bzm)$(dmso-S). − $C_{14}H_{18}Cl_2N_2O_3RuS$ (466.3): calcd. C 36.0, H 3.89, N 6.01; found C 36.0, H 3.77, N 6.00. − ^1H NMR ($CDCl_3$): δ = 2.44 and 2.42 (s, 3 H each, $B10H_3$ and $B11H_3$), 3.53 (s, 6 H, dmso-S), 3.86 (s, 3 H, $B12H_3$), 7.23 (s, 1 H, B7H), 7.37 (s, 1 H, B4H), 8.45 (s, 1 H, B2H). − Concentration of the mother liquor to a volume of 3 mL and addition of diethyl ether induced the precipitation of a second crop of white solid, which was likewise collected by filtration, washed with cold ethanol and diethyl ether, and dried in vacuo at room temperature (yield 60 mg, 40%). ^1H NMR analysis showed this second precipitate to consist of *c*,*c*,*c*-$RuCl_2(CO)_2(Me_3Bzm)_2$ slightly contaminated by the first product. Pure **7** was obtained by slow diffusion of methanol into a chloroform solution of the complex. − $C_{22}H_{24}Cl_2N_4O_2Ru$ (548.4): calcd. C 48.2, H 4.41, N 10.21; found C 48.0, H 4.40, N 10.18.

X-ray Diffraction: X-ray data were collected at room temperature [273(2) K] with an Enraf−Nonius CAD4 diffractometer using graphite-monochromated Mo-K_α radiation (λ = 0.71073 Å). The data were corrected for Lorentz and polarization effects by using a local program for data reduction. All the structures were solved by Patterson and Fourier methods,[22] and refined on F^2 by full-matrix least-squares methods.[23] Difference Fourier syntheses revealed the presence of a molecule of ethanol in **2** and of methanol in **5**, which were assigned occupancy factors of 0.5 on the basis of the Fourier peaks. Hydrogen atoms were placed in calculated positions (excluding those of the alcohol molecules in **2** and **5**) and were refined as riding, setting the U_{iso} to 1.2 × U_{eq} values of the parent carbon atoms. The crystal structure of the carbonyl derivative **5** is characterized by a disordered arrangement of the six-membered ring of the Me_3Bzm ligand [namely C(7)−C(10), C(20), C(21)] over two positions with statistical occupancy factors of 50%. Unit cell data and experimental conditions are summarized in Table 10. Crystallographic data (excluding structure factors) for the structures reported in this paper have been deposited with the Cambridge Crystallographic Data Centre and allocated the deposition numbers CCDC-139103−139108. Copies of the data can be obtained free of charge on application to the CCDC, 12 Union Road, Cambridge CB2 1EZ, U.K. [Fax: (internat.) + 44-1223/336-033; E-mail: deposit@ccdc.cam.ac.uk].

Molecular Mechanics: Calculations were performed with a Pentium 130 PC with the HyperChem 4.5 molecular modeling package[24] using the force field and procedures previously described for other Ru^{II}(sulfoxide complexes).[18] In calculating the electrostatic contributions, a distance-dependent relative permittivity was used. For the carbonyl derivatives, C and O charges were calculated by the semi-empirical method ZINDO/1 (C 0.33, O −0.10).[24] Stretching and bending force field constants involving the Ru−CO group, not included in the previous force field,[18] were calculated by Badger's rule, using the parameters given by Herschbach and Laurie,[25] and by Halgren's equation,[26] respectively. The following *d* and θ values were assumed: Ru−C 1.85 Å, C−O 1.14 Å, Ru−C−O 180°, X−Ru−C 90° and 180° for *cis* and *trans* X donors, respectively. Solvent-accessible surface areas were calculated by means of a HyperChem routine using a radius of 1.4 Å for the probe molecule.

Acknowledgments

This work was supported by the Italian MURST in the framework of the Project "Pharmacological and Diagnostic Properties of Metal Complexes" (coordinator Professor G. Natile). We thank Johnson Matthey for a loan of hydrated $RuCl_3$. P. A. M. acknowledges NIH grant GM 29222 for support.

[1] L. G. Marzilli, P. A. Marzilli, E. Alessio, *Pure Appl. Chem.* **1998**, *70*, 961−968.
[2] L. G. Marzilli, M. Iwamoto, E. Alessio, L. Hansen, M. Calligaris, *J. Am. Chem. Soc.* **1994** *116*, 815−816.
[3] E. Alessio, M. Calligaris, M. Iwamoto, L. G. Marzilli, *Inorg. Chem*. **1996**, *35*, 2538−2545.
[4] M. Iwamoto, E. Alessio, L. G. Marzilli, *Inorg. Chem*. **1996**, *35*, 2384−2389.
[5] E. Alessio, E. Zangrando, R. Roppa, L. G. Marzilli, *Inorg. Chem*. **1998**, *37*, 2458−2463.
[6] L. G. Marzilli, S. O. Ano, F. P. Intini, G. Natile, *J. Am. Chem. Soc.* **1999**, *121*, 9133−9142.
[7] A. H. Velders, A. C. G. Hotze, J. G. Haasnoot, J. Reedijk, *Inorg. Chem*. **1999**, *38*, 2762−2763.
[8] [8a]E. Alessio, L. Hansen, M. Iwamoto, L. G. Marzilli, *J. Am. Chem. Soc.* **1996**, *118*, 7593−7600. − [8b]E. Alessio, E. Zangrando, E. Iengo, M. Macchi, P. A. Marzilli, L. G. Marzilli, *Inorg. Chem.* **2000**, *39*, 294−303.
[9] The geometrical descriptors *cis*,*cis*,*cis*- (abbreviated *c*,*c*,*c*-) and *trans*,*cis*,*cis*- (abbreviated *t*,*c*,*c*-) refer to the relative geometries of pairs of ligands, either similar or dissimilar, in the order in which they appear in the chemical formula of the complex. See also Scheme 1.
[10] [10a] M. Calligaris, O. Carugo, *Coord. Chem. Rev.* **1996**, *153*, 83−154. − [10b] M. Calligaris, *Croat. Chem. Acta* **1999**, *72*, 147−169.
[11] E. Alessio, B. Milani, M. Bolle, G. Mestroni, P. Faleschini, F. Todone, S. Geremia, M. Calligaris, *Inorg. Chem.* **1995**, *34*, 4722−4734.
[12] The ^1H chemical shifts of Me_3Bzm ($CDCl_3$) in *c*,*c*,*c*-$RuCl_2$(dmso-S)$_2$(CO)(Me_3Bzm) and *cis*,*fac*-$RuCl_2$(dmso-S)$_3$(Me_3Bzm) are reported for the sake of comparison: *c*,*c*,*c*-$RuCl_2$(dmso-S)$_2$(CO)(Me_3Bzm): δ = 2.41 ($B11H_3$), 2.44 ($B10H_3$), 3.85 ($B12H_3$), 7.21 (B7H), 7.92 (B4H), 8.62 (B2H); *cis*,*fac*-$RuCl_2$(dmso-S)$_3$(Me_3Bzm): δ = 2.39 ($B10H_3$ and $B11H_3$), 3.87 ($B12H_3$), 7.21 (B7H), 7.87 (B4H), 8.82 (B2H). Peaks were assigned with the aid of NOESY spectra.
[13] E. Alessio, M. Macchi, S. L. Heath, L. G. Marzilli, *Inorg. Chem.* **1997**, *36*, 5614−5623.
[14] *Nomenclature of Inorganic Chemistry* (Ed.: G. L. Leigh), Blackwell, Oxford, U.K., **1990**; A. von Zelewsky, in *Stereochemistry of Coordination Compounds*, J. Wiley, Chichester, U.K., **1995**.
[15] J. D. Orbell, L. G. Marzilli, T. J. Kistenmacher, *J. Am. Chem. Soc*. **1981**, *103*, 5126−5133.
[16] S. Geremia, E. Alessio, F. Todone, *Inorg. Chim. Acta* **1996**, *253*, 87−90.
[17] E. Zangrando, F. Pichierri, L. Randaccio, B. Lippert, *Coord. Chem. Rev.* **1996**, *156*, 275−332.
[18] [18a] S. Geremia, M. Calligaris, *J. Chem. Soc., Dalton Trans.* **1997**, 1541−1547. − [18b] S. Geremia, L. Vicentini, M. Calligaris, *Inorg. Chem*. **1998**, *37*, 4094−4103. − [18c] S. Geremia, M. Calligaris, Yu. N. Kukushkin, A. V. Zinchenko, V. Yu. Kukushkin, *J. Mol. Struct.* **2000**, *516*, 49−56.
[19] M. Stener, M. Calligaris, *J. Mol. Struct. (Theochem)* **2000**, *497*, 91−104.
[20] E. Alessio, G. Mestroni, G. Nardin, W. M. Attia, M. Calligaris, G. Sava, S. Zorzet, *Inorg. Chem*. **1988**, *27*, 4099−4106.
[21] M. Henn, E. Alessio, G. Mestroni, M. Calligaris, W. M. Attia, *Inorg. Chim. Acta* **1991**, *187*, 39−50.

[22] G. M. Sheldrick, "SHELXS-86: Program for structure solution", *Acta Crystallogr.* **1990**, *A46*, 467−473.
[23] G. M. Sheldrick, *SHELXL-97: Program for crystal structure refinement*, University of Göttingen, Germany, **1997**.
[24] *HYPERCHEM*, Hypercube, Inc., Waterloo, Ont., Canada, **1994**.
[25] D. R. Herschbach, V. W. Laurie, *J. Chem. Phys.* **1961**, *35*, 458−463.
[26] T. A. Halgren, *J. Am. Chem. Soc.* **1990**, *112*, 4710−4723.
Received January 19, 2000
[I00019]